Diffractive lenses for chromatic confocal imaging

Sarah L. Dobson, Pang-chen Sun, and Yeshayahu Fainman

A diffractive zone plate provides a highly linear wavelength-to-depth coding, allowing for nonmechanical depth scanning in a confocal microscope. This chromatic confocal microscope, constructed with 40× and 60× objectives, achieves axial position changes of 55 and 25 μm, respectively, for a wavelength tuning range of 100 nm. The corresponding longitudinal point-spread functions are measured and shown to possess full-width half-maximums of 2.52 and 2.23 μm, respectively. Two-dimensional profiles of a two-phase-level grating and a four-phase-level diffractive structure are given. The performance of the chromatic confocal microscope is consistent with that of the conventional confocal operation of the microscope. © 1997 Optical Society of America

1. Introduction

The confocal scanning imaging technique is attractive for various microscopic imaging applications because of its capabilities of superior resolution,[1] rejection of scattered light,[2] and depth discrimination.[3] This method drew special interest in such applications as imaging biological samples and semiconductor materials, in which high definition in both the transverse and the longitudinal dimensions is required. The unique property of depth discrimination enables the confocal microscope to measure the profile of a three-dimensional (3-D) object by moving different parts of the object transversely and longitudinally into the focal region. The precision of the depth measurement depends on the point-spread function (PSF) in depth of the confocal imaging system as well as the depth resolution of the depth-scanning device. To achieve high depth resolution, most of the existing confocal imaging systems require a high precision and extremely stable mechanical scanning system.

Molesini *et al.*[4] developed an optical profilometer that uses the chromatic aberration of an optical system to provide focus-wavelength encoding for depth measurements. This method alleviates the requirement of mechanical depth scanning by allowing the different spectral components of the source to be focused onto different depth planes of the object. Following this notion, the chromatic confocal microscope employs a broadband light source (e.g., white-light source) and a dispersive objective lens for wavelength-to-depth coding.[5,6] The measured output power spectrum directly translates into the depth information of the object. Furthermore, the chromatic confocal microscope can perform parallel depth measurements by detecting and analyzing the output power spectrum components in parallel. It should be noted that chromatic confocal microscopes are suitable for applications that rely on reflection-mode operation.

Existing chromatic confocal microscopes suffer from technological limitations that need to be resolved. For example, commercially available microscope objective designs compensate for chromatic dispersion, thereby limiting the chromatic microscope scanning range. In addition, the dispersive properties of microscope objectives depend on the specific design and lens material characteristics, thus requiring individual calibration. Finally, the dispersion curve of the objective lens is usually nonlinear, resulting in wavelength-dependent sensitivity. In this paper we resolve these technological limitations by using a diffractive optical zone plate for wavelength-to-depth coding.[7] In contrast to the previous designs that use refractive elements, the diffractive element provides important features uniquely suitable for this application: (1) The dispersion resulting from diffraction phenomena is, in general, stronger than that from refraction, providing a more sensitive wavelength-to-depth coding; (2) the dispersion from the diffractive element is material independent and thus can be characterized analytically, allowing for calibration curves; (3) unlike reg-

The authors are with the Department of Electrical and Computer Engineering, University of California at San Diego, La Jolla, California 92093-0407.

Received 27 August 1996; revised manuscript received 9 December 1996.

0003-6935/97/204744-05$10.00/0

ular lenses that commonly contain surfaces of spherical shape to imitate parabolic phase functions and therefore possess certain spherical aberration, diffractive lenses do not possess the same aberration as they are coded with the exact parabolic phase function[8]; and (4) the diffractive element can be designed to compensate for or reduce the unwanted dispersion from the other optical elements in the same system, which is shown in our experiments. The only drawback of the diffractive lens is its limited numerical aperture (NA) that is constrained by the minimum feature size possible with current microfabrication technology. Such a small NA of the element limits its resolving power, making it unsuitable for use as the objective lens in a microscope. However, such a limitation does not restrict the use of the diffractive lens as an eyepiece in the microscope, which requires a rather low resolving power.

In this paper we address the properties and the advantages of the chromatic confocal microscope that employs a diffractive lens for wavelength-to-depth coding. In Section 2, the chromatic dispersion from a diffractive lens is analyzed and discussed in more detail. Section 3 begins with an outline of the experimental configuration and design of the chromatic confocal microscope and includes evaluation of the system characteristics: the wavelength-to-depth coding and the longitudinal PSF; it concludes with measurement profile results of two samples, a two-phase-level grating and a four-phase-level diffractive structure. The final section provides a summary and discussion of this research including some future research directions under investigation.

2. Chromatic Dispersion from the Diffractive Lens

Diffraction is naturally wavelength dependent, which is the biggest obstacle for applying diffractive elements in imaging because the strong chromatic dispersion of the element can completely ruin the image. However, in a chromatic confocal system, such strong chromatic dispersion of the diffractive element becomes the unique feature that helps to define focal spots through wavelength coding. The chromatic dispersion properties of a diffractive lens (e.g., a zone plate) can be characterized by the function of its focal length versus wavelength[9]:

$$f_m(\lambda) = \frac{r_1^2}{m\lambda}, \tag{1}$$

where m is the diffractive order, λ is the operating wavelength, and r_1 is the radius of the first zone. For the first diffractive order, the focal length of a diffractive lens follows the relation

$$f(\lambda) = f(\lambda_d)\,\frac{\lambda_d}{\lambda}, \tag{2}$$

where λ_d and $f(\lambda_d)$ are the design wavelength and the corresponding design focal length of the diffractive lens, respectively. Note that Eq. (2) depends on only the focal length for the design wavelength and is not affected by the material properties and type of the diffractive lens (i.e., amplitude or phase). Next we express Eq. (2) as a Taylor expansion around the design wavelength, giving the following relation:

$$f(\lambda) = \frac{f(\lambda_d)\lambda_d}{\lambda} = \sum_{n=0}^{\infty} (-1)^n f(\lambda_d)\left(\frac{\lambda - \lambda_d}{\lambda_d}\right)^n. \tag{3}$$

When the wavelength tuning range is much less than the design wavelength [i.e., $(\lambda - \lambda_d) \ll \lambda_d$], Eq. (3) can be approximated as a linear function when the higher-order terms are eliminated from the Taylor expansion, resulting in

$$f(\lambda) \approx f(\lambda_d)\left[1 - \left(\frac{\lambda - \lambda_d}{\lambda_d}\right)\right] = 2f(\lambda_d) + \frac{2(\lambda_d)}{\lambda_d}\lambda. \tag{4}$$

The diffraction efficiency of the element is determined by the number of phase quantization levels for the center wavelength and the slight dispersion of the material. The diffraction efficiency gradually decreases when the operating wavelength is tuned away from the design wavelength. For a sawtooth-profile phase grating, theory predicts a 2.7% efficiency reduction from its maximum value with wavelength changes 10% off the design wavelength.[10]

The diffractive optical element (DOE) used in our experiments was a four-phase-level diffractive lens designed to have a positive focal length of 250 mm at the design wavelength of 850 nm. A quartz wafer was first patterned by e-beam lithography and subsequently chemically etched in a hydrofluoric (HF) acid bath. The measured diffraction efficiency of the first diffraction order was ~80% at the design wavelength. With our design parameters, $\lambda_d = 850$ nm and $f(\lambda_d) = 250$ mm, approximation (4) becomes

$$f(\lambda)_{(\mathrm{mm})} = 500 - 0.294\lambda_{(\mathrm{nm})} \tag{5}$$

We experimentally measured the focal length of the zone plate over a total spectral range of 100 nm, from 800 to 900 nm. The linear-fit equation from the experimental data,

$$f(\lambda)_{(\mathrm{mm})} = 498.11 - 0.292\lambda_{(\mathrm{nm})} \tag{6}$$

follows Eq. (5) closely. The total focal-length change covered a range of ~29.2 mm. The deviation of the experimental data from the linear fit is ± 0.5 mm, which corresponds to 1.7% of the entire focal-length change.

3. Description of Experimental System

The experimental setup depicted in Fig. 1 is a confocal microscope system combined with the diffractive lens to introduce the wavelength-to-depth coding. A light beam from a tunable Ti:sapphire laser source is spatially filtered, expanded, and collimated. After passing through the beam splitter, the light beam is focused by the diffractive lens. The focus position $f(\lambda)$ of this focal point is determined by the operating wavelength, as expressed in approximation (6). The wave transmitted through the diffractive element is

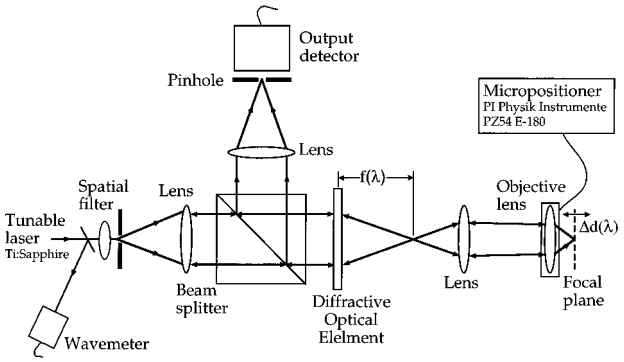

Fig. 1. Schematic diagram of a chromatic confocal microscope with a DOE.

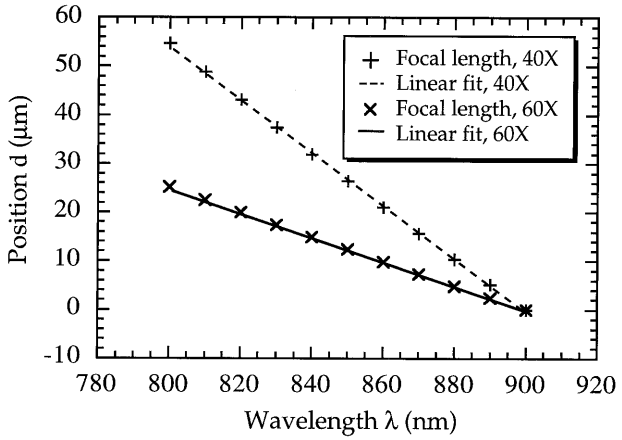

Fig. 2. Experimental results of system characterization: wavelength-to-depth mapping.

introduced into a telecentric imaging system composed of an achromatic lens with a focal length of 100 mm and a microscope objective. Two microscope objectives, 40× and 60×, were selected to characterize the performance of the confocal system. The 40× microscope objective from Oriel Corporation has a focal length of 4.5 mm and a NA of 0.65 at $\lambda = 850$ nm. The 60× microscope objective was manufactured by Olympus, and it has a focal length of 3.14 mm and a NA of 0.80 at $\lambda = 850$ nm. The telecentric system serves to image and demagnify the focus spot from the diffractive lens onto the object plane of the microscope objective, where the position of the focus is determined by the wavelength of the source. Because the aperture of the microscope objective of our system is fully illuminated, the lateral resolution is identical to that of the conventional confocal system when the same wavelength is being used. However, with the wavelength scanning range of 100 nm at a center wavelength of 850 nm, there will be a variation of the lateral resolution of approximately ±6% of that at a center wavelength. The demagnification enables a fine change of the focus position in depth by wavelength tuning, which can be characterized by a wavelength-to-depth coding. A sample introduced in the focus plane of the objective lens will reflect or scatter the optical wave back through the telecentric imaging system. After passing through the diffractive lens, the resultant collimated diffracted beam is redirected by the beam splitter and focused onto the output pinhole-detector assembly of the confocal microscope. The higher-order diffraction beams are focused onto different planes in the longitudinal direction and are significantly attenuated by the pinhole. The operating wavelength of the microscope was controlled by a mechanical tuner and monitored by a wavemeter (Burleigh Wavemeter$_{jr.}$, WA-2500) with a sensitivity of ±0.02 nm. Electro-optical tuning can also be implemented with high precision and at high speed. An additional power meter measured the input power into the system to provide power normalization at each wavelength. For comparison, we designed the system in such a way that it can also operate as a conventional confocal microscope. We achieved this by setting the source at a single wavelength, 850 nm (λ_d), and by employing a piezoelectric micropositioner assembly (PI Physik Instrumente, PZ54 E-180) used for mounting the microscope objective. The piezoelectric micropositioner provides mechanical depth scanning through axial movement of the microscope objective and, in turn, movement of the focal plane of the system. The micropositioner is capable of a 100-μm expansion for mechanical depth scanning with ±0.01-μm resolution.

4. Experimental System Characterization and Applications

For system characterization, we experimentally measured the wavelength-to-depth coding and the longitudinal PSF. The wavelength-to-depth coding, referred to as the wavelength-to-depth mapping, is expressed as a deviation d of the focal-point position, at a wavelength λ, from the focal point obtained at the design wavelength $\lambda_d = 850$ nm. The measurement result (see Fig. 2) shows, as predicted, a highly linear relation, with a constant sensitivity over a wavelength range of 100 nm around the design wavelength of 850 nm. A linear-curve fit of the experimental data gives the wavelength-to-depth mappings of the system for each microscope objective used, yielding

$$d_{40\times}(\lambda) = 490.91 - 0.546\lambda, \tag{7a}$$

$$d_{60\times}(\lambda) = 226.33 - 0.252\lambda. \tag{7b}$$

From Fig. 2, we can also see that with a wavelength tuning range of 100 nm, the focus position changes a total of 55 and 25 μm for the 40× and the 60× objectives, respectively. For each objective, the 40× and the 60×, respectively, the deviation of the experimental data from the linear fit is less than ±0.15 and ±0.48 μm, which corresponds to 0.6% and 0.8% of the entire depth position range. These results are better than those obtained from measurement of the diffractive zone plate alone [see approximation (6)]. This may occur because of the compensation between the higher-order chromatic dispersions (e.g., qua-

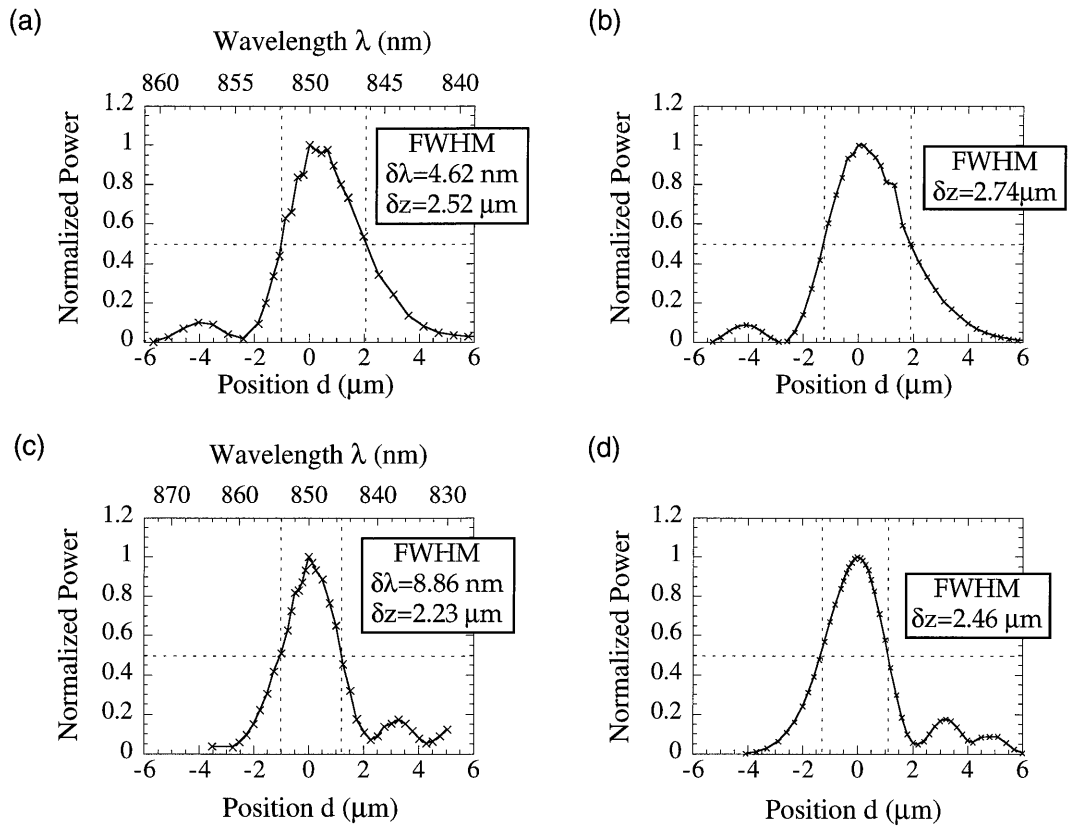

Fig. 3. Experimental results of the longitudinal PSF: chromatic confocal microscope with the (a) 40× objective, (c) 60× objective and the conventional confocal microscope operating at the design wavelength λ_d = 850 nm with the (b) 40× objective, (d) 60× objective.

dratic dependence) from the diffractive element and the refractive microscope objective.

The longitudinal PSF is an important parameter for characterization of confocal imaging systems in terms of depth resolution.[3] For the conventional confocal measurement, the longitudinal PSF is measured by the scanning of a mirror in depth through the focal plane of the objective and measurement of the output power from the detector. We obtained the longitudinal PSF for the chromatic confocal microscope in a similar way by placing a mirror in front of the focal plane of the objective lens (for a specific wavelength) and then measuring the output power while scanning the wavelength of the laser around that specific wavelength. Figure 3 shows the measurement results of the longitudinal PSF's for the chromatic and the conventional confocal systems. The FWHM values were calculated from a curve fit of the data. Longitudinal PSF's for confocal microscopes are characterized by intensity profiles approximated by a sinc-squared function.[2] From Fig. 3(a) for the 40× objective, we estimated a wavelength tuning FWHM of $\delta\lambda$ = 4.62 nm that corresponds to δz = 2.52 μm in depth. The FWHM value of the PSF with the piezoelectric micropositioner assembly in the conventional confocal system arrangement with the 40× objective and laser operation at the design wavelength λ_d = 850 nm is δz = 2.74 μm [see Fig. 3(b)]. Figure 3(c) illustrates the PSF for the chromatic confocal system with the 60× objective; the FWHM for the PSF is approximately $\delta\lambda$ = 8.86 nm, which corresponds to δz = 2.23 μm in depth. As depicted in Fig. 3(d), for the conventional confocal system with the 60× objective and laser operation at the design wavelength, the corresponding FWHM is δz = 2.46 μm. Again these values are in good agreement. In general, the conventional and the chromatic confocal microscopes have similar longitudinal PSF characteristics that provide comparable performance.

Finally, the chromatic confocal imaging system, illustrated in Fig. 1, was used to measure the surface profiles of two samples. The samples were measured by both chromatic and conventional confocal imaging schemes. In both cases, the transverse movement of the sample was accomplished by a simple translation stage with 1-μm resolution. The scanning in depth for the chromatic and the conventional confocal microscopes was achieved in the same manner as described in Section 3, i.e., the depth position of the sample was determined by the mechanical depth position (for the conventional confocal system) or the wavelength tuning (for the chromatic confocal system) in which the maximum intensity was detected through the pinhole.

Figure 4 illustrates the measured profiles of the

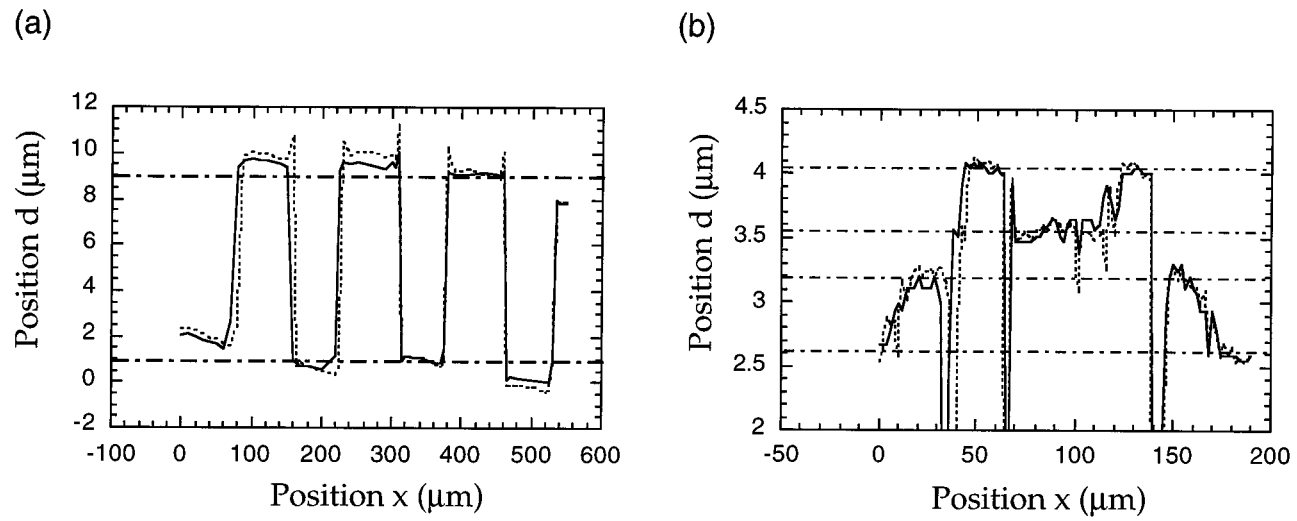

Fig. 4. Experimental results of measuring surface-relief profiles with the conventional (solid curves) and chromatic (dashed curves) confocal microscopes: (a) binary grating profile, (b) four-phase-level DOE. (The horizontal lines highlight the sample level positions.)

samples from the conventional confocal system (solid curves) and the chromatic confocal system (dashed curves). Figure 4(a) is the measured profile of a two-phase-level grating coated with a 20-nm thin film of Au to provide higher reflectivity. From the measured data, we estimate that the chromatic confocal method provides a grating depth of 8.5 μm, whereas the conventional confocal method provides a grating depth of 8.4 μm. Figure 4(b) illustrates the chromatic and the conventional confocal microscope profiles of a four-phase-level DOE. We suspect that the pronounced deep grooves appearing in Fig. 4(b) [not apparent in Fig. 4(a) because of a lower lateral sampling rate) are due to the sharp edges in the element that result in shadowing of the input illumination field and, consequently, misinterpretation of the signal at the output. In both cases, the profiles of the samples imaged with both the chromatic and the conventional confocal microscopes correspond well to each other.

5. Discussion and Summary

We demonstrate a chromatic confocal microscope that uses a diffractive lens for wavelength-to-depth coding and nonmechanical depth scanning. Our method provides such advantages as nonmechanical depth scanning, high linearity, and high sensitivity in wavelength-to-depth mapping. The chromatic confocal microscope was characterized in terms of the measured longitudinal PSF and the scanning range provided by wavelength-to-depth mapping curves. Finally, sample profiles were measured experimentally, and the results were found to be in good agreement with those obtained with the conventional confocal microscope.

There are many possible improvements and specific changes in application to our chromatic confocal microscope that are under investigation. In the future, we intend to incorporate an electro-optic wavelength scanner for high-speed depth scanning and to explore the use of a compact tunable semiconductor laser source. Likewise, a broadband source and parallel array detectors can be used to make parallel depth measurements possible. In order to perform parallel lateral measurements, a multi-phase-level diffractive element array will be introduced into the system. In addition, we are exploring the applications of our chromatic confocal system for writing and reading 3-D bit-oriented optical memories and for biological 3-D imaging.

The authors thank Fang Xu and Rob Stein for preparing the DOE and providing the measurement sample. The research is funded by the U.S. National Science Foundation.

References

1. T. Wilson and S. J. Hewlett, "Superresolution in confocal scanning microscopy," Opt. Lett. **16,** 1062–1064 (1991).
2. T. Wilson and C. Sheppard, *Theory and Practice of Scanning Optical Microscopy* (Academic, London, 1984).
3. D. K. Hamilton, T. Wilson, and C. J. R. Sheppard, "Experimental observations of depth-discrimination properties of scanning microscopes," Opt. Lett. **6,** 625–626 (1981).
4. G. Molesini, G. Pedrini, P. Poggi, and F. Quercioli, "Focus-wavelength encoded optical profilometer," Opt. Commun. **49,** 229–233 (1984).
5. M. A. Browne, O. Akinyemi, and A. Boyde, "Confocal surface profiling utilizing chromatic aberration," Scanning **14,** 145–153 (1992).
6. M. Maly and A. Boyde, "Real-time stereoscopic confocal reflection microscopy using objective lenses with linear longitudinal chromatic dispersion," Scanning **16,** 187–192 (1994).
7. M. C. Hutley and R. F. Stevens, "The use of a zone-plate monochromator as a displacement transducer," J. Phys. E **21,** 1037–1044 (1988).
8. J. N. Mait, "Understanding diffractive optic design in the scalar domain," J. Opt. Soc. Am. A **12,** 2145–2158 (1995).
9. R. D. Guenther, *Modern Optics* (Wiley, New York, 1990).
10. G. S. Swanson, "Binary optics technology: the theory and design of multi-level diffractive optical elements," MIT Lincoln Laboratory Tech. Rep. **854,** (MIT, Cambridge, Mass., 1989).